Available online at www.sciencedirect.com
SCIENCE DIRECT®
C. R. Biologies 328 (2005) 767–772
COMPTES RENDUS BIOLOGIES
http://france.elsevier.com/direct/CRASS3/

Medical sciences / Sciences médicales

A method to quantify at late imaging a release rate of ^{18}F-FDG in tissues

Éric Laffon [a,b,*], Michèle Allard [a], Roger Marthan [b], Dominique Ducassou [a]

[a] *Service de médecine nucléaire, hôpital du Haut-Lévêque, centre hospitalo-universitaire de Bordeaux, av. de Magellan, 33600 Pessac, France*
[b] *Laboratoire de physiologie cellulaire respiratoire, Inserm E356, université Bordeaux-2, 33076 Bordeaux, France*

Received 16 November 2004; accepted after revision 21 June 2005

Available online 2 August 2005

Presented by Jean Rosa

Abstract

This theoretical work shows that the rate constant for the ^{18}F-FDG release in tissues can be assessed without needing any arterial blood sampling. The method requires that the clearance of ^{18}F-FDG from plasma has occurred, whereas ^{18}F-FDG is still present in the tissue. This condition can be met dating from 3 h after ^{18}F-FDG injection, when hydration and/or phlorizin injection are applied after the routine static acquisition. The release rate constant can be obtained from a graphical analysis performed at the later decreasing phase of the tissue tracer activity. A two-compartment and a three-compartment model are developed, both in accordance with one another. ***To cite this article: É. Laffon et al., C. R. Biologies 328 (2005).***
© 2005 Académie des sciences. Published by Elsevier SAS. All rights reserved.

Résumé

Une méthode de quantification aux temps tardifs d'une libération du ^{18}F-FDG par les tissus. Le principe d'une quantification du taux de libération du ^{18}F-FDG par un tissu ne nécessitant pas de prélèvement de sang artériel est présenté. La méthode est valide lorsque la disparition du traceur du plasma est intervenue, alors que le traceur est toujours présent dans le tissu. Cette condition peut être remplie 3 h après l'injection du traceur, avec une hydratation et/ou l'injection de phlorizine pratiquées après l'acquisition statique de routine. Le taux de libération peut être alors obtenu par une analyse graphique de la phase tardive de la courbe d'activité du ^{18}F-FDG dans le tissu. Deux modèles sont proposés, à deux puis à trois compartiments, qui sont en accord. ***Pour citer cet article : É. Laffon et al., C. R. Biologies 328 (2005).***
© 2005 Académie des sciences. Published by Elsevier SAS. All rights reserved.

Keywords: PET; ^{18}F-FDG release; Kinetic modelling; k_4

Mots-clés : TEP ; Relaxation du ^{18}F-FDG ; Modèle cinétique ; k_4

* Corresponding author.
E-mail address: elaffon@u-bordeaux2.fr (É. Laffon).

1631-0691/$ – see front matter © 2005 Académie des sciences. Published by Elsevier SAS. All rights reserved.
doi:10.1016/j.crvi.2005.06.004

1. Introduction

Assuming that the 2-[^{18}F]fluoro-2-deoxy-D-glucose (^{18}F-FDG) is trapped in cancer cells in an irreversible manner, PET-scan allows quantification of the metabolic rate of glucose in tumours, by several methods that aimed at quantifying the ^{18}F-FDG uptake rate [1–5]. Is the irreversibility of the ^{18}F-FDG uptake an oversimplification? Usually, most biological reactions do not occur in a completely irreversible manner, which has been clearly established in neuroreceptor quantification models [6]. Moreover, in the particular case of ^{18}F-FDG PET imaging, the tracer metabolism by hepatic tumours challenges this notion of irreversibility [7]. A first quantification method of the ^{18}F-FDG release rate constant has been proposed by Phelps et al. [8], as an extension of Sokoloff's model [1]. Then, Patlak has proposed a graphical method for reversible tracers [2], as an extension of his previous method for irreversible ones. These latter methods both require a dynamic acquisition, which is achieved during the first hour after the tracer injection, and an invasive blood tracer sampling.

The aim of this theoretical work is to propose a graphical method allowing for the assessment of the ^{18}F-FDG release in tissues, on certain conditions, but without needing any blood tracer sampling. It is an extension of a recently published method that aimed at quantifying the rate constant for an irreversible tracer uptake [5]. It requires the acquisition of a dynamic PET scan at the later decreasing phase of the tissue tracer activity. Both a two-compartment and a three-compartment model are developed, and simulated data are provided.

2. Two-compartment model

Let us consider the ^{18}F-FDG uptake from blood to an intracellular compartment (Fig. 1a). The ^{18}F-FDG uptake rate constant is K, and the ^{18}F-FDG release rate constant is k_B. At the steady state, the rate of trapped tracer per tissue volume unit dC_T/dt is:

$$dC_T/dt = K C_P(t) - k_B C_T(t) - \lambda C_T(t) \quad (1)$$

where $C_P(t)$ represents the tracer concentration in the plasma, and λ is the ^{18}F physical decay constant ($\lambda = \ln 2/110\ \text{min}^{-1}$).

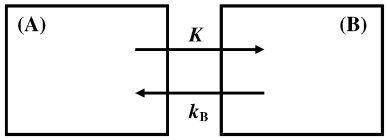

a

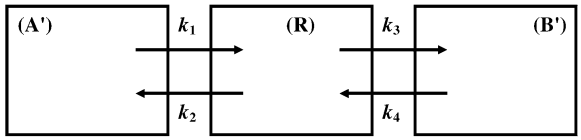

b

Fig. 1. (**a**) The two-compartment model roughly considers compartments (**A**) and (**B**), which involve blood free ^{18}F-FDG and ^{18}F-FDG trapped in intracellular cytoplasm, respectively. The ^{18}F-FDG uptake and release rate constants, K and k_B, respectively, are the transport rate constants between the two compartments. (**b**) In comparison with the two-compartment model, the three-compartment model introduces an intermediate reversible compartment (R), which considers free ^{18}F-FDG in interstitial fluid and intracellular cytoplasm. The rate constants k_1 and k_2 account for forward and reversed transport between compartments (A′) and (R), respectively. The rate constants k_3 and k_4 account for forward and reversed transport between compartments (R) and (B′), i.e. for ^{18}F-FDG phosphorylation by hexokinase and ^{18}F-FDG-6-PO$_4$ dephosphorylation by G-6-phosphatase, respectively.

In patients with a normal renal and hepatic function, the time duration required to reach the steady state is estimated to last about 5 min [3], and the amount of the tracer that accumulates in the tissue during this time duration is assumed to be negligible in comparison with that which accumulates during the whole examination. Moreover, for simplicity, let us assume that the ^{18}F-FDG blood time-activity curve (TAC) exponentially decays with a mean constant α, after the peak (see simulated data for a multiexponential decay). In a nearly similar manner to that used in a previous work on ^{18}F-FDG (irreversible) uptake [5], when $t = 0$ is set at the blood tracer peak, the solution of Eq. (1) is:

$$C_T(t) = K C_P(t=0)\left[e^{-(\lambda+k_B)t} - e^{-\alpha t}\right]/(\alpha - \lambda - k_B) \quad (2)$$

Eq. (2) is very similar to that of a radioactive chain equation, but with a whole decay constant equal to $\lambda + k_B$. When $e^{-(\lambda+k_B)t}$ is much greater than $e^{-\alpha t}$, i.e. when the clearance of ^{18}F-FDG from plasma has occurred whereas ^{18}F-FDG is still present in the tis-

sue, the later phase of the trapped tracer TAC can be approximated by:

$$\lambda C_T(t) \cong \lambda K C_P(t=0)\, e^{-(\lambda+k_B)t}/(\alpha-\lambda-k_B) \quad (3)$$

Eq. (3) shows that a single exponential fitting to the later phase of the ^{18}F-FDG TAC can provide the release rate constant k_B, since λ is known, without needing any arterial blood sampling. (If an arterial blood sampling is carried out, a graphical analysis can also provide the ^{18}F-FDG uptake rate constant K [5].) Let us note that, at the later phase of the tracer activity in the tissue: (*i*) neglecting the part of the tracer amount accumulated in the tissue during the time duration to reach the steady state is justified, since both ^{18}F physical decay and ^{18}F-FDG release have occurred, and (*ii*) $\lambda C_T(t)$ actually corresponds to the measured trapped ^{18}F-FDG activity, since the blood ^{18}F-FDG is negligible (see simulated data). Furthermore, Eq. (2) allows us to predict that the time T_m corresponding to the maximal ^{18}F-FDG activity in the tissue is lower than that estimated when no ^{18}F-FDG release occurs (T'_m) [5]:

$$T_m = \ln\big[\alpha/(\lambda+k_B)\big]/\big[\alpha-(\lambda+k_B)\big] \quad (4)$$

$$T'_m = \ln[\alpha/\lambda]/[\alpha-\lambda] \quad (5)$$

3. Three-compartment model

In a three-compartment model (Fig. 1b), the ^{18}F-FDG transport rate constants between the compartments are different from those of a two-compartment model (Fig. 1a). However, relationships can be established [2]:

$$K = k_1k_3/(k_2+k_3) \quad (6)$$

$$k_B = k_4k_2/(k_2+k_3) \quad (7)$$

Following Patlak [2], let us suppose that k_4 is much lower than the other rate constants of the system. Furthermore, let us consider measurements are started up at the later phase of the ^{18}F-FDG activity in the tissue, when the clearance of ^{18}F-FDG from plasma has occurred whereas ^{18}F-FDG is still present in the tissue, in other words, when the tracer uptake from the blood into the tissue is much lower than the tracer release from the tissue. Thereby, when the tracer uptake from the blood into the tissue can be ignored, the rate of change of trapped tracer per tissue volume unit dC_T/dt is:

$$dC_T(t)/dt = k_3C_{rev}(t) - k_4C_T(t) - \lambda C_T(t) \quad (8)$$

where C_{rev} is the free ^{18}F-FDG in the tissue. The rate of change of the free tracer per tissue volume unit $dC_{rev}(t)/dt$ is:

$$dC_{rev}(t)/dt = k_4C_T(t) - k_3C_{rev}(t) - k_2C_{rev}(t) - \lambda C_{rev}(t) \quad (9)$$

The *whole* solutions of Eqs. (8) and (9) are, respectively:

$$C_T(t) = C_{T_0}\, e^{-(\lambda+k_4)t} + k_3\, e^{-(\lambda+k_4)t}] \times \int_0^t C_{rev}(\tau)\, e^{(\lambda+k_4)\tau}\, d\tau \quad (10)$$

$$C_{rev}(t) = C_{R_0}\, e^{-(\lambda+k_2+k_3)t} + k_4\, e^{-(\lambda+k_2+k_3)t}] \times \int_0^t C_T(\tau)\, e^{(\lambda+k_2+k_3)\tau}\, d\tau \quad (11)$$

where C_{T0} and C_{R0} are constants representing trapped and free ^{18}F-FDG concentration in the tissue at the beginning of the measurement, respectively. This measurement start, i.e. $t = 0$ in the three-compartment model, occurs at the steady state of the later decreasing phase of the tissue tracer TAC, i.e. when the tracer uptake from the blood into the tissue is much lower than the tracer release from the tissue, hence when C_{rev} mainly depends on the release of trapped tracer. Consequently, (a) in Eq. (10) the second term of the right-hand side is much lower than the first one (also see below), (b) in Eq. (11) (representing the *whole* solutions of Eq. (9)), the first term of the right-hand side is not relevant and can be cancelled. Thus, introducing Eq. (10) in Eq. (11) yields the following solution for free ^{18}F-FDG in the tissue, when the second order term is neglected:

$$C_{rev}(t) \cong k_4\, e^{-(\lambda+k_2+k_3)t} \times \int_0^t C_{T_0}\, e^{-(\lambda+k_4)\tau+(\lambda+k_2+k_3)\tau}\, d\tau \quad (12)$$

Then, integrating Eq. (12) leads to:

$$C_{\mathrm{rev}}(t) \cong \left[k_4/(k_2+k_3-k_4)\right] C_{\mathrm{T}_0} \times \left[\mathrm{e}^{-(\lambda+k_4)t} - \mathrm{e}^{-(\lambda+k_2+k_3)t}\right] \quad (13)$$

hence, since $k_4 \ll k_2 + k_3$:

$$C_{\mathrm{rev}}(t) \cong \left[k_4/(k_2+k_3)\right] C_{\mathrm{T}_0}\, \mathrm{e}^{-(\lambda+k_4)t} \quad (14)$$

This result justifies that in Eq. (10) the second term of the right-hand side can be considered much lower than the first one. Furthermore, introducing Eq. (14) into Eq. (10) and rearranging yields the following expression for the trapped tracer activity:

$$\lambda C_{\mathrm{T}}(t) \cong \lambda C_{\mathrm{T}_0}\, \mathrm{e}^{-(\lambda+k_4)t}(1+k_{\mathrm{R}}t) \quad (15)$$

$$k_{\mathrm{R}} = k_4 k_3/(k_2+k_3) \quad (16)$$

where k_{R} can be considered a ^{18}F-FDG 'retrapping' rate constant, by comparison with Eq. (6). Eq. (15) also approximates the measured tissue activity, since the part of the free tracer activity can be considered to be negligible in comparison with that of the trapped tracer.

Furthermore, Eq. (17) hereafter shows that the transport rate constants available from Eqs. (15) and (16), k_4 and k_{R} in a three-compartment model, are in agreement with that available from Eq. (3), k_{B} in a two-compartment model:

$$\mathrm{e}^{-(\lambda+k_{\mathrm{B}})t} = \mathrm{e}^{-(\lambda+k_4-k_{\mathrm{R}})t} \cong \mathrm{e}^{-(\lambda+k_4)t}[1+k_{\mathrm{R}}t] \quad (17)$$

4. Simulated data

The proposed two-compartment model assumes, for simplicity, that the ^{18}F-FDG blood TAC decays with a mean constant α. However, it has been shown that the ^{18}F-FDG plasma clearance was multi-exponential, i.e. that the input function (IF) was three-exponential [9]. When such an IF is taken into account, Eq. (2) becomes:

$$C_{\mathrm{T}}(t) = \sum_{i=1}^{3} K A_i \left(\mathrm{e}^{-(\lambda+k_{\mathrm{B}})t} - \mathrm{e}^{-\alpha_i t}\right)/(\alpha_i - \lambda - k_{\mathrm{B}}) \quad (18)$$

Fig. 2 shows simulated data from Eq. (18) and references [9,10], for different values of k_{B} and α_3. At the later phase of the ^{18}F-FDG TAC, when $\exp[-(\lambda + k_{\mathrm{B}})t]$ is much greater than $\exp[-\alpha_i t]$, a single exponential fitting can provide the ^{18}F-FDG release rate

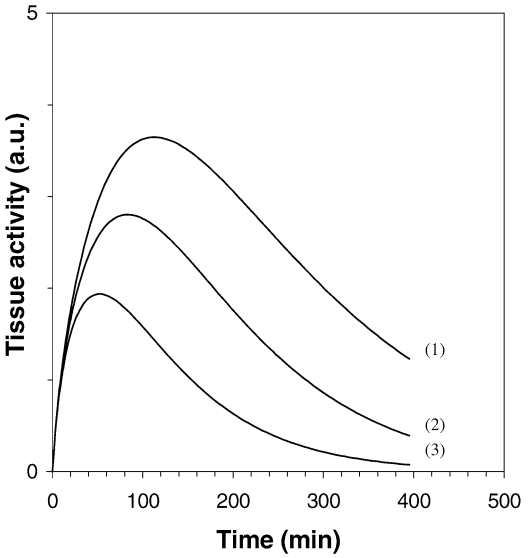

Fig. 2. Simulation of the tissue ^{18}F-FDG TAC in a two-compartment model (Eq. (18)), for different values of α_3 and k_{B} [9–11]: (1) $\alpha_3 = 0.0109$, $k_{\mathrm{B}} = 0\,\mathrm{min}^{-1}$; (2) $\alpha_3 = 0.0109$, $k_{\mathrm{B}} = 0.0050\,\mathrm{min}^{-1}$; (3) $2.25 \times \alpha_3 = 0.0245$, $k_{\mathrm{B}} = 0.0050\,\mathrm{min}^{-1}$. The axis origin is set at the blood tracer TAC peak (not shown).

constant k_{B}, since λ is known, without needing any arterial blood sampling. One hour after injection, in comparison with $\lambda + k_{\mathrm{B}} = 0.0113\,\mathrm{min}^{-1}$ [10], the two first IF exponential constants satisfy this condition, $\alpha_1 = 1.568\ \mathrm{min}^{-1}$ and $\alpha_2 = 0.1438\ \mathrm{min}^{-1}$ [9], but not $\alpha_3 = 0.0109\ \mathrm{min}^{-1}$ [9].

The greater the constant α_3, the faster the tracer plasma clearance 1 h after injection, the earlier the implementation of the method. This feature highlights the major part of hydration and/or phlorizin injection [11,12], which should be made in practice from the end of the routine static acquisition to the beginning of the dynamic acquisition, in order to increase α_3. It has been shown indeed that phlorizin injection resulted in an increase by a factor of 2.25 in the plasma clearance rate of ^{18}F-FDG in rats, and that urinary excretion of ^{18}F-FDG in phlorizin-treated rats was very near that of hydrated rats [11]. Consequently, assuming that at least the condition:

$$\exp\left[-(\lambda+k_{\mathrm{B}})t\right] = 10 \times \exp[-\alpha_3 t] \quad (19)$$

is required, when α_3 is increased to a value of $2.25 \times 0.0109 = 0.0245\ \mathrm{min}^{-1}$, the time landmark t_{l} to apply the proposed method is about 3 h after ^{18}F-FDG injection.

From data involved in curve 3 of Fig. 2 ($k_B = 0.0050$ and $\alpha_3 = 0.0245$ min^{-1}, i.e. with hydration and/or phlorizin injection), single exponential fittings to the 180–240, 240–300, 300–360, and 360–420-min time ranges lead to estimates of k_B equal to 0.0042, 0.0046, 0.0048 and 0.0049 min^{-1}, respectively, which should be compared with the value of 0.0050 min^{-1}. Note that curve 2 in Fig. 2 ($k_B = 0.0050$ and $\alpha_3 = 0.0109$ min^{-1}, i.e. without hydration and/or phlorizin injection), leads in the 360–420-min time range to an (under)estimate of 0.0023 min^{-1}.

5. Discussion

Without needing any blood tracer sampling, when hydration and/or phlorizin injection are applied after the routine static PET acquisition, a two-compartment model analysis allows us to quantify the ^{18}F-FDG release rate constant k_B from a dynamic acquisition occurring at about 3 h after ^{18}F-FDG injection. The later the dynamic acquisition, the more accurate the k_B estimate, but, the greater the ^{18}F-FDG release from the tissue, the more underestimated the value of k_B. Moreover, this theoretical work presents a three-compartment model analysis, which supports the two-compartment one, and allows us to differentiate between the rate constants for ^{18}F-FDG dephosphorylation and rephosphorylation, k_4 and k_R, respectively. The principle of the present model analysis could be applied to other ^{18}F-labelled tracers than the ^{18}F-FDG, at the later decreasing phase of the tissue TAC, when the clearance of the tracer from plasma has occurred whereas it is still present in the tissue.

From Eq. (18) and literature data [9–11], Fig. 2 shows quite different ^{18}F-FDG tissue TACs, related to different values of k_B and of the late IF exponential constant α_3. To the very best of our knowledge, the later decreasing phase of ^{18}F-FDG tissue TACs and the significant parts of k_B and α_3 have not been studied so far. It is suggested that, given the limited understanding of tumour metabolism, in addition to the quantification of the ^{18}F-FDG uptake, the quantification of the ^{18}F-FDG release could be investigated to characterize tumours, to differentiate malignant processes from infectious or inflammatory processes [13], and to assess the effects of treatment [7]. Furthermore, Patlak's graphical analysis for assessing ^{18}F-FDG release rate constant requires an invasive arterial blood sampling and the acquisition of a dynamic PET scan that are performed during the first hour after the tracer injection [2–4]. In contrast, a similar assessment that can be obtained from the proposed graphical analysis appears to be easier to implement in a busy clinical environment, since it is non-invasive and requires a dynamic acquisition that occurs far from the static acquisition.

In conclusion, the principle of a graphical analysis that aimed at quantifying the rate constant for ^{18}F-FDG release in tissues is presented, which is an extension of a recently published method for assessing the tracer uptake rate [5]. This whole method emphasizes the interest of the later decreasing phase of the ^{18}F-FDG activity in tissues.

Acknowledgement

The authors wish to thank Schering-CISbiointernational for helpful discussion, and H. Dupouy and I. Hessling for technical assistance. They also thank an anonymous reviewer for his comments on the manuscript.

References

[1] L. Sokoloff, M. Reivich, C. Kennedy, M.H. Des Rosiers, C.S. Patlak, K.D. Pettigrew, O. Sakurada, M. Shinohara, The |^{14}C]deoxyglucose method for the measurement of local cerebral glucose utilization: theory, procedure, and normal values in the conscious and anesthetized albino rat, J. Neurochem. 28 (1977) 897–916.

[2] C.S. Patlak, R.G. Blasberg, Graphical evaluation of blood-to-brain transfer constants from multiple-time uptake data: generalizations, J. Cereb. Blood Flow Metab. 5 (1985) 584–590.

[3] N. Sadato, T. Tsuchida, S. Nakamura, A. Waki, H. Uematsu, N. Takahashi, N. Hayashi, Y. Yonekura, Y. Ishii, Non-invasive estimation of the net influx constant using the standardized uptake value for quantification of FDG uptake of tumours, Eur. J. Nucl. Med. 25 (1998) 59–564.

[4] N.M. Freedman, S.K. Sundaram, K. Kurdziel, J.A. Carrasquillo, M. Whatley, J.M. Carson, D. Sellers, S.K. Libutti, J.C. Yang, S.L. Bacharach, Comparison of SUV and Patlak slope for monitoring of cancer therapy using serial PET scans, Eur. J. Nucl. Med. 30 (2003) 46–53.

[5] E. Laffon, M. Allard, R. Marthan, D. Ducassou, A method to quantify the uptake rate of 2-[^{18}F]fluoro-2-deoxy-D-glucose in tissues, Nucl. Med. Commun. 25 (2004) 851–854.

[6] M. Ichise, J.-H. Meyer, Y. Yonekura, An introduction to PET and SPECT neuroreceptor quantification models, J. Nucl. Med. 42 (2001) 755–763.
[7] S. Okazumi, K. Isono, K. Enomoto, T. Kituchi, M. Osaki, H. Yamamoto, H. Hayashi, T. Asano, M. Ryu, Evaluation of liver tumors using fluorine-18-fluorodeoxyglucose PET: characterization of tumor and assessment of effect of treatment, J. Nucl. Med. 33 (1992) 333–339.
[8] M.E. Phelps, S.C. Huang, E.J. Hoffman, C. Selin, L. Sokoloff, D.E. Kuhl, Tomographic measurement of local cerebral glucose metabolic rate in humans with (F-18)2-fluoro-2-deoxy-D-glucose: validation of method, Ann. Neurol. 6 (1979) 371–388.
[9] S. Eberl, A.R. Anayat, R.R. Fulton, P.K. Hooper, M.J. Fulham, Evaluation of two population-based input functions for quantitative neurological FDG PET studies, Eur. J. Nucl. Med. 24 (1997) 299–304.
[10] L.G. Strauss, A. Dimitrakopoulou-Strauss, D. Koczan, L. Bernd, U. Haberkorn, V. Ewerbeck, H.-J. Thiesen, ^{18}F-FDG kinetics and gene expression in giant cell tumors, J. Nucl. Med. 45 (2004) 1528–1535.
[11] J.K. Moran, H.B. Lee, M.D. Blaufox, Optimization of urinary FDG excretion during PET imaging, J. Nucl. Med. 40 (1999) 1352–1357.
[12] J.R.L. Ehrenkranz, N.G. Lewis, C.R. Kahn, J. Roth, Phlorizin: a review, Diabetes Metab. Res. Rev. 21 (2005) 31–38.
[13] A. Matthies, M. Hickeson, A. Cuchiara, A. Alavi, Dual time point ^{18}F-FDG PET for the evaluation of pulmonary nodules, J. Nucl. Med. 43 (2002) 871–875.